

**AFRL-ML-WP-TP-2007-424**

**MICROSTRUCTURE OF DENSE THIN  
SHEETS OF  $\gamma$ -TiAl FABRICATED BY  
HOT ISOSTATIC PRESSING OF TAPE-  
CAST MONOTAPES (PREPRINT)**



**A.G. Adams, M.N. Rahaman, and Rollie E. Dutton**

**FEBRUARY 2007**

**Approved for public release; distribution unlimited.**

**STINFO COPY**

**The U.S. Government is joint author of this work and has the right to use, modify,  
reproduce, release, perform, display, or disclose the work.**

**MATERIALS AND MANUFACTURING DIRECTORATE  
AIR FORCE RESEARCH LABORATORY  
AIR FORCE MATERIEL COMMAND  
WRIGHT-PATTERSON AIR FORCE BASE, OH 45433-7750**

# REPORT DOCUMENTATION PAGE

*Form Approved  
OMB No. 0704-0188*

The public reporting burden for this collection of information is estimated to average 1 hour per response, including the time for reviewing instructions, searching existing data sources, gathering and maintaining the data needed, and completing and reviewing the collection of information. Send comments regarding this burden estimate or any other aspect of this collection of information, including suggestions for reducing this burden, to Department of Defense, Washington Headquarters Services, Directorate for Information Operations and Reports (0704-0188), 1215 Jefferson Davis Highway, Suite 1204, Arlington, VA 22202-4302. Respondents should be aware that notwithstanding any other provision of law, no person shall be subject to any penalty for failing to comply with a collection of information if it does not display a currently valid OMB control number. **PLEASE DO NOT RETURN YOUR FORM TO THE ABOVE ADDRESS.**

<b>1. REPORT DATE (DD-MM-YY)</b> February 2007			<b>2. REPORT TYPE</b> Journal Article Preprint		<b>3. DATES COVERED (From - To)</b>		
<b>4. TITLE AND SUBTITLE</b>  MICROSTRUCTURE OF DENSE THIN SHEETS OF $\gamma$ -TiAl FABRICATED BY HOT ISOSTATIC PRESSING OF TAPE-CAST MONOTAPES (PREPRINT)			<b>5a. CONTRACT NUMBER</b> F33615-01-D-5801-0032				
			<b>5b. GRANT NUMBER</b>				
			<b>5c. PROGRAM ELEMENT NUMBER</b> 63112F				
<b>6. AUTHOR(S)</b>  A.G. Adams and M.N. Rahaman (University of Missouri-Rolla) Rollie E. Dutton (AFRL/MLLM)			<b>5d. PROJECT NUMBER</b> 4349				
			<b>5e. TASK NUMBER</b> L0				
			<b>5f. WORK UNIT NUMBER</b> T2				
<b>7. PERFORMING ORGANIZATION NAME(S) AND ADDRESS(ES)</b>			<b>8. PERFORMING ORGANIZATION REPORT NUMBER</b>				
University of Missouri-Rolla Department of Materials Science and Engineering 223 McNutt Hall Rolla, MO 65409		Metals Branch (AFRL/MLLM) Metals, Ceramics and NDE Division Materials and Manufacturing Directorate Air Force Research Laboratory, Air Force Materiel Command Wright-Patterson AFB, OH 45433-7750					
<b>9. SPONSORING/MONITORING AGENCY NAME(S) AND ADDRESS(ES)</b>  Materials and Manufacturing Directorate Air Force Research Laboratory Air Force Materiel Command Wright-Patterson AFB, OH 45433-7750			<b>10. SPONSORING/MONITORING AGENCY ACRONYM(S)</b> AFRL-ML-WP				
			<b>11. SPONSORING/MONITORING AGENCY REPORT NUMBER(S)</b> AFRL-ML-WP-TP-2007-424				
<b>12. DISTRIBUTION/AVAILABILITY STATEMENT</b> Approved for public release; distribution unlimited.							
<b>13. SUPPLEMENTARY NOTES</b>  Journal article submitted to Materials Science and Engineering.  The U.S. Government is joint author of this work and has the right to use, modify, reproduce, release, perform, display, or disclose the work. PAO Case Number: AFRL/WS 07-0403; Date cleared: 26 Feb 2007.							
<b>14. ABSTRACT</b>  A powder metallurgy route based on hot isostatic pressing (HIPing) of tape-cast monotapes was used for the direct fabrication of dense thin sheets of gamma titanium aluminide. Polarized light microscopy revealed a fine-grained microstructure but a few isolated larger grains were also present. The primarily metastable $\alpha_2$ microstructure of the rapidly solidified starting powder transformed to the equilibrium near-gamma microstructure during HIPing. Chemical analysis revealed that the dense sheet had a carbon content of 0.13 wt.%, which was only 0.04 wt.% higher than that of the starting powder, but the oxygen content was significantly higher, presumably introduced during the decanning step. The hardness measured using Vickers microindentation technique was 384 + 9 HV. Manipulation of the as-HIPed microstructure was performed by heating for up to 1 hour in flowing argon at temperatures below and above the alpha transus. Below 1250 °C, limited grain growth and no discernable change in the as-HIPed (near-gamma) microstructure occurred.							
<b>15. SUBJECT TERMS</b> gamma titanium aluminide, thin sheet, tape casting, hot isostatic pressing							
<b>16. SECURITY CLASSIFICATION OF:</b>			<b>17. LIMITATION OF ABSTRACT:</b> SAR		<b>18. NUMBER OF PAGES</b> 38	<b>19a. NAME OF RESPONSIBLE PERSON (Monitor)</b> Rollie E. Dutton <b>19b. TELEPHONE NUMBER (Include Area Code)</b> N/A	
<b>a. REPORT</b> Unclassified	<b>b. ABSTRACT</b> Unclassified	<b>c. THIS PAGE</b> Unclassified					

# Microstructure of dense thin sheets of $\gamma$ -TiAl fabricated by hot isostatic pressing of tape-cast monotapes

A.G. Adams<sup>1</sup>, M.N. Rahaman<sup>1,\*</sup>, R. E. Dutton<sup>2</sup>

<sup>1</sup>University of Missouri-Rolla, Department of Materials Science and Engineering, 223 McNutt Hall, Rolla, MO 65409

<sup>2</sup>Air Force Research Laboratory, Materials and Manufacturing Directorate, Wright-Patterson AFB, OH 45433

## Abstract

A powder metallurgy route based on hot isostatic pressing (HIPing) of tape-cast monotapes was used for the direct fabrication of dense thin sheets (250–300  $\mu\text{m}$  thick) of gamma titanium aluminide ( $\gamma$ -TiAl). Polarized light microscopy revealed a fine-grained microstructure (average grain size  $\sim 3 \mu\text{m}$ ) but a few isolated larger grains ( $\sim 20 \mu\text{m}$ ) were also present. The primarily metastable  $\alpha_2$  microstructure of the rapidly solidified starting powder transformed to the equilibrium near- $\gamma$  microstructure during HIPing. Chemical analysis revealed that the dense sheet had a carbon content of 0.13 wt.%, which was only 0.04 wt.% higher than that of the starting powder, but the oxygen content was significantly higher, presumably introduced during the decanning step. The hardness measured using Vickers microindentation technique was  $384 \pm 9 \text{ HV}$ . Manipulation of the as-HIPed microstructure was performed by heating for up to 1 hour in flowing argon at temperatures (1170–1385°C) below and above the alpha transus (1355°C). Below 1250°C, limited grain growth and no discernable change in the as-HIPed (near- $\gamma$ ) microstructure occurred. Sheets heated to 1320°C and 1365°C had a duplex microstructure of  $\gamma$  and  $\alpha_2$  grains, with some lamellar grains. Except for a thin surface layer (20–30  $\mu\text{m}$  thick), the microstructure of the heat-treated sheet was uniform, but a fully lamellar microstructure was not achieved even after heating for 1 h at 1385°C.

**Keywords:** gamma titanium aluminide; thin sheet, tape casting, hot isostatic pressing.

\*Corresponding author. Tel.: 573-341-4406; fax: 573-341-6934

E-mail address: rahaman@umr.edu (M.N. Rahaman).

## 1. Introduction

Intermetallic alloys based on gamma titanium aluminide ( $\gamma$ -TiAl) possess several attractive properties such as low density, strength retention to high temperatures, high strength-to-weight ratio, high stiffness, and good oxidation resistance [1-3]. These properties make  $\gamma$ -TiAl a potentially attractive material for high-temperature space and aerospace applications. For several applications,  $\gamma$ -TiAl sheets and foils are needed with thicknesses as low as 100  $\mu\text{m}$ . These sheets are being considered for applications such as exhaust nozzle components, back structures of scramjets for space applications, heat shields for helicopters, and thermal protection systems for reusable launch vehicles [4].

Several methods have been developed for fabricating  $\gamma$ -TiAl sheets but only one, the Advanced Sheet Rolling Process (ASRP) developed by Plansee AG (Austria), reached production scale. Because of the low ductility of  $\gamma$ -TiAl at ambient temperatures, conventional production methods are based on thermomechanical processing of ingot or powder metallurgy material at temperatures above 1100°C. The ASRP is a modified pack-rolling process pioneered at Battelle Memorial Institute and the Air Force Research Laboratory [5,6] which allows nearly isothermal processing on a conventional hot rolling mill at temperatures within the  $\alpha + \gamma$  phase field and at low rolling speeds [7-9]. Microstructural inhomogeneity and low yield are key problems with sheets produced by the ingot-metallurgy rolling process [9-16]. The large amount of thermomechanical treatment required for microstructural homogeneity coupled with the low yield makes the sheets very expensive [10,11]. The use of powder-metallurgy plate as a starting material for the rolling process leads to a reduction of the aforementioned problems of low yield and microstructural inhomogeneity [4,16,17], but the production of  $\gamma$ -TiAl sheet by this method is still uneconomical.

Recently, Rahaman et al. [18] investigated the feasibility of using a powder-metallurgy route based on hot isostatic pressing (HIPing) of tape-cast monotapes for the direct production of dense thin sheets of  $\gamma$ -TiAl without the need for hot working. A powder produced by the plasma rotating electrode process (PREP<sup>TM</sup>) was mixed with an organic binder and a solvent to form a slurry, which was tape cast to produce a green sheet. After insertion of the green sheet into a HIP can and binder burnout in situ, densification was achieved by HIPing at 1100°C and 130 MPa for 15 minutes. Following a decanning step, a dense sheet (thickness = 250–300  $\mu\text{m}$ ) with a duplex microstructure was obtained. The areal dimensions of the sheet, 50 mm by 20 mm, were limited by the size of the HIP vessel.

The objective of the present work was to characterize the microstructure and properties of  $\gamma$ -TiAl sheet fabricated by the process developed by Rahaman et al. [18], using HIPing of tape-cast sheets. A gas atomized powder was used in the present work because of its availability. Manipulation of the as-HIPed microstructure by thermal annealing at temperatures between 1170°C and 1385°C was performed to determine the range of microstructures that can be developed from the HIPed sheets.

## 2. Experimental procedure

### 2.1 Starting Powder

The  $\gamma$ -TiAl powder used in the present experiments was kindly provided by Crucible Materials Corp., Pittsburgh, PA. It was produced by a gas atomization process. The powder provided was the alloy designated 395MM. It had a composition Ti-46.6Al-2.2Nb-1.3Cr-0.3Mo-0.211B-0.305C (at.%). Particle size analysis (Beckman-Coulter LS 230; Coulter Corp., Miami,

FL) and scanning electron microscopy, SEM (JEOL 330) were used to characterize the average size, size distribution, morphology and structure of the starting powder.

## 2.2 Fabrication of Dense Sheets by HIPing

The fabrication process consisted of the following steps: preparation of green sheets by tape casting, encapsulation of the sheet in a HIP can, *in situ* binder burnout, HIPing, and decanning. The tape-casting and HIPing procedures were generally similar to those described by Rahaman et al. [18], but the use of a different starting powder meant that some modification of the tape casting procedure was necessary. In addition, the binder burnout and decanning steps were modified to make them more compatible with production methods for potential industrial application. In the tape-casting step, a stock solution of the binder–plasticizer mixture was first prepared by dissolving 100 g of B-72 resin (Rohm & Haas Co., Philadelphia, PA) and 20 g of dibutyl phthalate (Fisher Scientific, Fairlawn, NJ) in 200 g of methyl ethyl ketone, MEK (Reagent grade; Sigma-Aldrich, St. Louis, MO). Next, a slurry was prepared by mixing 50 g of  $\gamma$ -TiAl powder, 2.6 g of the binder–plasticizer mixture, and  $\sim$  8 cm<sup>3</sup> of MEK. The slurry was cast using a tape caster with a fixed carrier surface and a movable doctor blade, on a flat surface that was covered with Teflon sheet to facilitate removal of the tape after drying. A doctor blade gap of 1.0 mm and a casting speed of 40 cm/min were used. The tape was allowed to dry for approximately 30 min and then peeled off from the Teflon film.

The size of the HIP vessel used in the experiments limited the dimensions of the HIPed sheet to  $\sim$  5 cm  $\times$  2 cm. A green tape was inserted into a HIP can, consisting of a commercial-purity Ti frame enclosed within a mild steel can. The contact surfaces of the Ti frame with the

tape cast sheet and with the mild steel can were separated with Ta foil to prevent reaction and eutectic melting. Binder burnout was performed *in situ* by flowing Ar into one end of the can and pulling a small vacuum at the other end with a vacuum pump while the sample was heated at 1°C/min to 450°C, with a holding time of 30 min at 250°C, 300°C, 350°C, and 400°C. It was held at 450°C for two hours and then cooled to room temperature at a rate of 5°C/min. Following the binder burnout step, the HIP can was heated to 300°C, evacuated, and sealed. HIPing was performed for 15 min at 1100°C and 130 MPa. The heating and cooling rates were 20°C/min.

To remove the dense sheet from the HIP can, the area containing the  $\gamma$ -TiAl was removed from the rest of the can by wire cutting, and placed in an acid bath to dissolve the mild steel. The Ta foil separators were then oxidized away by heating for 12–24 h in air at 700°C (heating and cooling rates = 5°C/min).

### *2.3 Characterization of Starting Powder and HIPed Sheets*

The carbon and oxygen content of the starting powder, the tape cast monotape after debinding, and the dense sheet produced by HIPing were analyzed by a commercial laboratory (LECO Corporation, St. Joseph, MI). The small size of the sheet and the amount of material needed for other experiments meant that the only measurement of mechanical properties that could be done was microindentation hardness. Vickers microindentation technique (LECO DM-400 Hardness Tester) was used to measure the hardness of the dense sheet, with an applied load of 1 kgf. Ten measurements were taken along the centerline of the sheet.

Metallographic sections of the atomized powder were prepared by sprinkling a small quantity of powder into a mold filled with epoxy resin, and allowing the particles to fall to the

bottom of the mold before the epoxy hardened. The sample was then ground on 180, 240, 320, 400, and 600 grit SiC papers. Polishing was performed with 15  $\mu\text{m}$  diamond paste for 3 h, 1  $\mu\text{m}$  diamond suspension on a Buehler Vibromet polisher for 4 h, and Buehler Mastermet colloidal silica suspension on a Buehler Vibromet polisher overnight ( $\sim$ 16 h). Metallographic sections of the HIPed  $\gamma$ -TiAl sheet were prepared by mounting samples in thermosetting resin, then using the same grinding and polishing procedure described for the atomized powder.

The microstructures of the polished cross sections were observed in a polarized light optical microscope and in a scanning electron microscope, SEM (Hitachi S-570) with a backscattered electron detector. Grain size was measured from the optical micrographs using the linear intercept method [19]. The mean intercept length  $L$  was determined from the equation:

$$L = \frac{L_T}{M N_T} \quad (1)$$

where  $L_T$  is the total length of the lines,  $M$  is the magnification of the micrographs, and  $N_T$  is the sum of the grains counted from all lines. Measurements were made for  $N_T > 200$ . A 95% confidence level for the mean intercept length was determined using the equation:

$$\Delta L = \frac{1.2L}{\sqrt{2N_T}} \quad (2)$$

The average grain size  $G$  and the 95% confidence level ( $\Delta G$ ) were determined from the equations:

$$G = 1.74L \quad (3)$$

$$\Delta G = 1.74\Delta L \quad (4)$$

## 2.4 Heat Treatment of as-HIPed Sheet

The effect of heat treatment on the microstructure of the as-HIPed sheet was studied by heating the sheet at temperatures in the  $\alpha + \gamma$  and  $\alpha$  phase fields [2]. The  $\alpha$  transus temperature of the 395MM alloy used in this work was reported as 1355°C [20]. Heat treatments were performed in flowing Ar (60 cm<sup>3</sup>/min) for 12 min and 1 h at 1170°C, 1245°C, 1320°C, and 1365°C. These were the actual temperatures near the sample, measured using a Type S thermocouple. The heat treatment temperatures are shown in Figure 1 on a Ti–Al phase diagram taken from Reference 2. Titanium sponge was used as an oxygen getter in the furnace. A heating rate of 5°C/min was used, and the samples were furnace cooled at ~10°C/min. Preparation of metallographic sections of the heat-treated samples and observations of the microstructure were performed using the procedures described earlier.

## 3. Results and Discussion

### 3.1 Powder Characteristics

The particle size distribution of the  $\gamma$ -TiAl powder is shown in Figure 2. The distribution had a mean size of 60  $\mu\text{m}$  and a standard deviation of 20  $\mu\text{m}$ . The distribution consisted primarily of one major peak centered at approximately the mean value, but there was a minor peak centered about ~120  $\mu\text{m}$ , approximately twice the mean size. SEM images revealed that the starting powder particles were primarily spherical with a few ligamental and irregular particles (Figure 3). Backscattered electron imaging of the particle cross-section (Figure 4) showed a cellular–dendritic structure of the rapidly-solidified, gas atomized powder. The cell size varied between 2  $\mu\text{m}$  and 10  $\mu\text{m}$ . Typically, as the atomized powder solidifies, the  $\alpha$  phase is the first

solid phase to form from the undercooled liquid. The interdendritic regions solidify by peritectic reaction to form the  $\gamma$  phase.

### 3.2 Characteristics of Tape-Cast and HIPed Sheets

Figure 5 shows the fractured cross-section of a  $\gamma$ -TiAl tape after binder burnout and pre-sintering (1 h at 1000°C in vacuum) to provide adequate strength for handling. The thickness of the tape was 700  $\mu\text{m}$ . The particle packing density appeared to be homogeneous across the length and thickness of the cross-section. A complete sheet after HIPing and decanning is shown in Figure 6(a). The dimensions were approximately 5 cm  $\times$  1.5 cm. An optical micrograph of the polished cross-section (Figure 6(b)) showed that the tape was fully dense, with a nearly uniform cross-section of  $\sim$ 275  $\mu\text{m}$ .

The carbon and oxygen contents at three stages of the sheet fabrication process are given in Table 1. Compared to the starting powder, the C content of the tape-cast monotape after debinding increased by 0.02 wt.%, with a further increase of 0.02 wt.% after HIPing and decanning. The data indicated that the fabrication process did not lead to any significant C contamination of the material. The O content of the tape after debinding was only 0.02 wt.% greater than that of the starting powder. However, the O content increased to 0.44 wt.% after HIPing and decanning. This significant increase in the O content was due presumably to the oxidation stage of the decanning process, when the adherent Ta foil was removed by oxidation in air for 24 hr at 700°C. Removing a thin surface layer by lightly grinding the sheet with SiC paper resulted in a reduction in the O content of the sheet to 0.33 wt.%, indicating that the oxygen was concentrated near the surface. Thermogravimetric analysis, performed subsequently,

indicated that the time for complete oxidation of the Ta foil separators used in the experiments (thickness = 0.005 inch) was less than 3 h at 700°C, compared to a time of 12–24 h used in the decanning experiments. Optimization of the oxidation step in decanning, coupled with surface finishing to better remove the surface oxide layer, might be expected to produce a significant reduction in the O content of the final sheet.

The hardness of the dense HIPed sheet was  $384 \pm 9$  HV. Two of the indents are shown in [Figure 7](#). Fan-shapes regions of deformation were observed around the indents, indicating that some plastic flow occurred. This suggests that the material produced by the present process may have the ability to develop a limited amount of ductility for subsequent forming into a complex shape.

### *3.3 Microstructure of the Dense as-HIPed $\gamma$ -TiAl Sheet*

Polarized light optical microscopy ([Figure 8\(a\)](#)) showed that the dense as-HIPed  $\gamma$ -TiAl sheet had a fine-grained microstructure with an average grain size of  $3.4 \pm 0.2$   $\mu\text{m}$ . This microstructure is very similar to the fine, equiaxed, near- $\gamma$  microstructure reported recently [[20,21](#)] for large compacts of the same alloy produced by HIPing at temperatures between 1000°C and 1300°C. A fine-grained microstructure is very desirable for subsequent microstructural manipulation of  $\gamma$ -TiAl to optimize its properties for the desired application. Heat treatment would be required to produce a microstructure suitable for applications where high temperature properties and good toughness are needed.

Detailed examination of the polished cross-section of the dense sheet indicated the presence of a few large grains ( $\sim 20$   $\mu\text{m}$ ) in the fine-grained microstructure ([Figure 8\(b\)](#)).

Approximately five regions of large grains were observed in a total cross-section of  $\sim 2$  cm by 250-300  $\mu\text{m}$ . These large grains re-entered the normal size distribution after subsequent heat treatment of the as-HIPed sheet at temperatures greater than 1250°C. A few explanations may be suggested for the presence of these large grains in the as-HIPed microstructure. It is possible that the large  $\gamma$  grains originated from the interdendritic regions of powder particles that were cooled at a slower rate and thus had a larger scale of segregation. This segregation can lead to regions of  $\gamma$  grains without  $\alpha_2$  grains to pin the grain boundaries [22]. Large particles cool slower, so removing the largest powder particles could reduce or eliminate this effect. However, slow-cooled particles are not necessarily large. Although the homogeneity of gas atomized powder is better than that produced by other methods, microsegregation during solidification can still occur. Other possible causes include nonuniformities in chemical composition. Aluminum segregation could place the local composition slightly to the right of the peritectic, which increases the likelihood of forming interdendritic  $\gamma$  phase. The borides that are used to pin grain boundaries could also be nonuniformly distributed. Lack of borides in these regions could explain the presence of the larger grains [22].

### 3.4 Microstructural Manipulation of as-HIPed $\gamma$ -TiAl Sheet

Figure 9(a) and Figure 9(b) show polarized light optical micrographs of the HIPed  $\gamma$ -TiAl sheet after heating for 12 min at 1320°C and 1365°C, respectively. The  $\alpha$  transus temperature (1355°C) reported for the 395MM alloy used in this work [20] is between these two temperatures. The average grain sizes of the heat-treated samples, determined from polarized

light optical micrographs, are summarized in [Table 2](#). The grains grew from an as-HIPed average grain size of  $\sim 3 \mu\text{m}$  to an average of  $\sim 20 \mu\text{m}$  after the heat treatment for 1 h at  $1375^\circ\text{C}$ .

Backscattered electron imaging was used to observe the phases present in the microstructures after heat treatment. The as-HIPed sheet, as well as those heated at  $1170^\circ\text{C}$  and  $1245^\circ\text{C}$ , had a near- $\gamma$  structure. They contained primarily  $\gamma$  grains with  $\alpha_2$  at grain boundaries and triple points. Based on the results of previous work [[1,2,20](#)], near- $\gamma$  was the expected microstructure after the  $1170^\circ\text{C}$  heat treatments, but a duplex microstructure was expected after the  $1245^\circ\text{C}$  treatments. The samples heated at  $1320^\circ\text{C}$  and  $1365^\circ\text{C}$  had a duplex microstructure, with  $\gamma$  and  $\alpha_2$  grains as well as grains with very coarse lamellae ([Figure 10\(a\)](#) and [Figure 10\(b\)](#)). In previous work, it was observed that heating at temperatures just below the  $\alpha$  transus typically produced a nearly lamellar microstructure, whereas heating above the  $\alpha$  transus produced a fully lamellar structure [[1,2,20,21](#)]. In the present work, neither the sheet heated for 1 h at  $1320^\circ\text{C}$  nor that heated for 1 h at  $1365^\circ\text{C}$  formed the amount of lamellar grains that was observed in previous work [[20,21](#)]. After heat treatment at  $1320^\circ\text{C}$ , only a few of these lamellar grains were seen, but many more were found after treatment for 1 h at  $1365^\circ\text{C}$  ([Figure 11\(a\)](#)). Heating for 1 h at  $1385^\circ\text{C}$ , well above the  $\alpha$  transus, produced a large increase in the amount of lamellar grains ([Figure 11\(b\)](#)), but a fully lamellar microstructure was still not observed even after this heat treatment. In a HIPed compact of the same alloy, a fully lamellar microstructure was obtained after only 30 min at  $1360^\circ\text{C}$  [[20,21](#)].

Surface effects were seen in the HIPed sheets that were heated at the highest temperatures. [Figure 12](#) shows the lamellar surface of a sheet heated for 12 min at  $1365^\circ\text{C}$ . The thickness of this lamellar surface region was  $20\text{-}30 \mu\text{m}$ . The formation of this lamellar surface

region was likely due to the oxygen contamination of the surface. Oxygen is an  $\alpha$  stabilizer. By promoting the  $\alpha$  phase, it therefore promoted the formation of lamellar grains when the sheet was cooled from high temperature. The major source of such oxygen contamination was the air present during the oxidation of the Ta foil during the decanning step (12–24 h at 700°C). Except for the thin surface layer, the microstructure of the sheet was very uniform (Figure 9 to Figure 11). No significant gradient in phase composition or grain size was observed in the interior of the sheet between the thin surface layers. If surface oxide contamination of the as-HIPed sheet cannot be eliminated prior to heat treatment, a quick grinding step afterward would be expected to produce a uniform product. For this reason, the microstructure of the interior of the sheet is of far more importance than the surface effects.

#### 4. Conclusions

A powder-metallurgy route involving tape-casting, *in situ* binder burnout, and hot isostatic pressing (HIPing) for 15 min at 1100°C and under 130 MPa pressure produced dense sheets of  $\gamma$ -TiAl with a thickness of 250–300  $\mu\text{m}$ . Chemical analysis indicated that the dense HIPed sheet had a carbon content (0.13 wt.%) after decanning, which was only 0.04 wt.% higher than that of the starting powder. The oxygen content of the HIPed sheet was much higher than the values for the powder and for the tape after binder burnout, presumably caused by oxidation during the decanning step. The hardness of the HIPed sheet measured using Vickers microindentation technique was  $384 \pm 9$  HV. Polarized light microscopy revealed that the as-HIPed sheet had a fine-grained, near- $\gamma$  microstructure (average grain size  $\sim 3 \mu\text{m}$ ) but a few larger grains ( $\sim 20 \mu\text{m}$ ) were also observed in isolated regions of the cross-section. Heat treatment of the as-HIPed sheet

produced commonly-observed microstructures. A sheet heated for up to 1 h at 1170°C and 1245°C had a near- $\gamma$  microstructure similar to the as-HIPed sheet, whereas a sheet heated for 1 h at 1320°C and 1365°C had a duplex microstructure of  $\gamma$  and  $\alpha_2$  grains, with several coarse lamellar grains. Heating for 1 h at 1385°C produced a predominantly lamellar structure. Whereas oxygen contamination influenced the microstructure of a thin surface region (20-30  $\mu\text{m}$ ) of the sheet, particularly after the higher temperature heat treatments, no microstructural gradients were seen in the interior of the sheets, indicating that a uniform sheet could be produced after reduction of the oxygen contamination or removal of the thin surface layer.

**Acknowledgements:** This work was funded by the Air Force Research Laboratory (TOPS DO Contract Number 0032). The authors would like to thank S. L. Semiatin, P. L. Martin, A. H. Rosenberger, and D. C. Van Aken for helpful suggestions and technical discussions. The assistance of T. Brown and J. Murry for assistance with hot isostatic pressing, and E. Fletcher and D.C. Van Aken with optical microscopy is gratefully acknowledged. The authors would also like to thank Crucible Materials Corporation, Pittsburgh, PA, for providing the  $\gamma$ -TiAl powder used in the experiments.

## References

- [1] Y.-W. Kim, Intermetallic alloys based on gamma titanium aluminide, JOM 41 (1989) 24-30.
- [2] Y.-W. Kim, D.M. Dimiduk, Progress in the understanding of gamma titanium aluminides, JOM 43 (1991) 40-47.

- [3] F.H. Froes, C. Suryanarayana, D. Eliezer, Review: synthesis, properties and applications of titanium aluminides, *J. Mater. Sci.* 27 (1992) 5113-5140.
- [4] G. Das, P.A. Bartolotta, H. Kestler, H. Clemens, The development of sheet gamma TiAl technology under the enabling propulsion materials/high speed civil transport (EPM/HSCT) program, in: Y.-W. Kim, H. Clemens, A. H. Rosenberger (Eds.), *Gamma Titanium Aluminides* 2003, TMS, Warrendale, PA, 2003, pp. 33-45.
- [5] S. L. Semiatin, Wrought processing of ingot metallurgy gamma titanium aluminide alloys, in: Y.-W. Kim, R. Wagner, M. Yamaguchi (Eds.), *Gamma Titanium Aluminides*, TMS, Warrendale, PA, 1995, pp. 509-524.
- [6] S.L. Semiatin, S.M. El-Soudani, D.C. Vollmer, C.R. Thompson, Thermomechanical processing of ingot metallurgy near gamma titanium aluminides to refine grain size and optimize mechanical properties, US patent 5,442. 847, August 1995.
- [7] H. Clemens, W. Glatz, P. Schretter, C. Koeppe, A. Bartels, R. Behr, A. Wanner, Processing and mechanical properties of  $\gamma$ -TiAl based alloy sheet material, in: Y.-W. Kim, R. Wagner, M. Yamaguchi (Eds.), *Gamma Titanium Aluminides*, TMS, Warrendale, PA, 1995, pp. 717-726.
- [8] C. Koeppe, A. Bartels, H. Clemens, P. Schretter, W. Glatz, Optimizing the properties of TiAl sheet material for application in heat protection shields or propulsion systems, *Mater. Sci. Eng. A* 201 (1995) 182-193.
- [9] H. Clemens, Intermetallic  $\gamma$ -TiAl based alloy sheet materials – processing and mechanical properties, *Z. Metallkd.* 86 (1995) 814-822.
- [10] J.H. Moll, B.J. McTiernan, PM TiAl alloys: the sky's the limit, *Metal Powder Report*, 55 (2000) 18-22.

- [11] S.L. Semiatin, J.C. Chestnutt, C. Austin, V. Seetharaman, Processing of intermetallic alloys, in: M.V. Nathal, R. Darolia, C.T. Liu, P.L. Martin, D.B. Miracle, R. Wagner, M. Yamaguchi (Eds.), Structural Intermetallics 1997, TMS, Warrendale, PA, 1997, pp. 263-276.
- [12] S.L. Semiatin, G.R. Cornish, D. Eylon, Hot-compression behavior and microstructure evolution of pre-alloyed powder compacts of a near- $\gamma$  titanium aluminide alloy, Mater. Sci. Eng. A185 (1994) 45-53.
- [13] S.L. Semiatin, P.A. McQuay, Segregation and homogenization of a near-gamma titanium aluminide, Metall. Trans. 23A (1992) 149-161.
- [14] S.L. Semiatin, R. Nekkanti, M.K. Alam, P.A. McQuay, Homogenization of near-gamma titanium aluminides: analysis of kinetics and process scaleup feasibility, Metall. Trans. 24A (1993) 1295-1306.
- [15] U. Habel, C.F. Yolton, J.H. Moll, Gas-atomized  $\gamma$ -titanium aluminide based alloys – processing, microstructure, and mechanical properties, in: Y.-W. Kim, D.M. Dimiduk, M.H. Loretto (Eds.), Gamma Titanium Aluminides 1999, TMS, Warrendale, PA, 1999, pp. 301-306.
- [16] G. Das, H. Kestler, H. Clemens, P.A. Bartolotta, Sheet gamma TiAl: status and opportunities, JOM 56 (2004) 42-45.
- [17] J.P. Beckman, H. Clemens, P. Schretter, W. Glatz, P.E. Jones, D. Eylon, C.F. Yolton, Effect of processing on properties of rolled gamma titanium aluminide sheet made from powder metallurgy plate, in: P.A. Blenkinsop, W.J. Evans, H.N. Flower (Eds.), Titanium '95: Science and Technology, Woodhead Publishing, Cambridge, UK, 1996, pp. 217-225.
- [18] M.N. Rahaman, R. E. Dutton, S.L. Semiatin, Fabrication of dense thin sheets of  $\gamma$ -TiAl by hot isostatic pressing of tape-cast monotapes, Mater. Sci. Eng. A360 (2003) 169-175.

- [19] H.E. Exner, Qualitative and quantitative surface microscopy, in: R.W. Cahn and P. Haasen (Eds.), Physical Metallurgical, 3<sup>rd</sup> ed., Elsevier Science, New York, 1983, pp. 581-647.
- [20] U. Habel, G. Das, C.F. Yolton, Y.-W. Kim, Processing, microstructure and tensile properties of  $\gamma$ -TiAl PM alloy 395MM, in: Y.-W. Kim, H. Clemens, A. H. Rosenberger (Eds.), Gamma Titanium Aluminides 2003, TMS, Warrendale, PA, 2003, pp. 297-304.
- [21] C.F. Yolton, Y.-W. Kim, U. Habel, Powder metallurgy processing of gamma titanium aluminide, in: Y.-W. Kim, H. Clemens, A. H. Rosenberger (Eds.), Gamma Titanium Aluminides 2003, TMS, Warrendale, PA, 2003, pp. 233-240.
- [22] S.L. Semiatin, Private communication.

Table 1

Impurity content at three stages of the  $\gamma$ -TiAl sheet fabrication process

Stage of process	C (wt.%)	O (wt.%)
$\gamma$ -TiAl powder	0.09	0.08
Tape after debinding	0.11	0.11
HIPed sheet after decanning	0.13	0.44

Table 2

Average grain size and 95% confidence level of HIPed  $\gamma$ -TiAl sheet after annealing for times  $t = 12$  min and  $t = 1$  h at various isothermal temperatures. (As-HIPed grain size =  $3.4 \pm 0.2$   $\mu\text{m}$ )

Annealing temperature ( $^{\circ}\text{C}$ )	Grain size ( $\mu\text{m}$ )	
	$t = 12$ min	$t = 1$ h
1170	$4.9 \pm 0.3$	$5.7 \pm 0.3$
1245	$5.1 \pm 0.3$	$5.7 \pm 0.4$
1320	$7.8 \pm 0.5$	$7.8 \pm 0.5$
1365	$13.9 \pm 0.8$	$20.2 \pm 1.2$

## Figure captions

Figure 1. Part of the Ti–Al phase diagram, taken from Reference 2, showing the composition of the starting powder, the HIPing temperature ( $1100^{\circ}\text{C}$ ), and the heat treatment temperatures of the as-HIPed sheet: A =  $1170^{\circ}\text{C}$ ; B =  $1245^{\circ}\text{C}$ ; C =  $1320^{\circ}\text{C}$ ; D =  $1365^{\circ}\text{C}$ .

Figure 2. Particle size distribution of the gas atomized  $\gamma$ -TiAl starting powder (alloy 395MM).

Figure 3. SEM image of  $\gamma$ -TiAl starting powder consisting of primarily spherical particles, with a few ligamental and irregular particles.

Figure 4. Backscattered electron image of the cross-section of the  $\gamma$ -TiAl starting powder, showing cellular  $\alpha_2$  phase (lighter phase) with  $\gamma$  phase (darker phase) in the interdendritic regions.

Figure 5. Fractured cross-section of tape-cast  $\gamma$ -TiAl sheet after binder burnout and pre-sintering (1 h at  $1000^{\circ}\text{C}$  in vacuum).

Figure 6. (a) Complete dense  $\gamma$ -TiAl sheet, after HIPing and decanning; (b) optical micrograph of the cross-section of the dense  $\gamma$ -TiAl sheet, with a thickness of  $\sim 275 \mu\text{m}$ .

Figure 7. Optical micrograph showing Vickers microindents along the cross-section of a dense  $\gamma$ -TiAl sheet. Regions of deformation (arrowed) were observed around the indents.

Figure 8. Polarized light optical micrograph of as-HIPed  $\gamma$ -TiAl sheet: (a) with an average grain size of  $\sim 3 \mu\text{m}$ , and (b) showing the presence of a few large grains with a size of  $\sim 20 \mu\text{m}$  (arrowed) in a predominantly fine-grained matrix.

Figure 9. Polarized light optical micrographs of HIPed  $\gamma$ -TiAl sheet after heating for 12 min at (a)  $1320^{\circ}\text{C}$ , and (b)  $1365^{\circ}\text{C}$ .

Figure 10. Backscattered electron image of HIPed  $\gamma$ -TiAl sheet heated for (a) 1 h at 1320°C, and (b) 12 min at 1365°C, showing a duplex microstructure of  $\gamma$  grains (dark phase) and  $\alpha_2$  grains (light phase), with some lamellar grains (arrowed).

Figure 11. Polarized light optical micrographs of HIPed  $\gamma$ -TiAl sheet heated for 1 h at (a) 1365°C, and (b) at 1385°C. A fully lamellar microstructure was not achieved even at 1385°C.

Figure 12. Backscattered electron image of the near surface region of HIPed  $\gamma$ -TiAl sheet heated for 12 min at 1365°C.

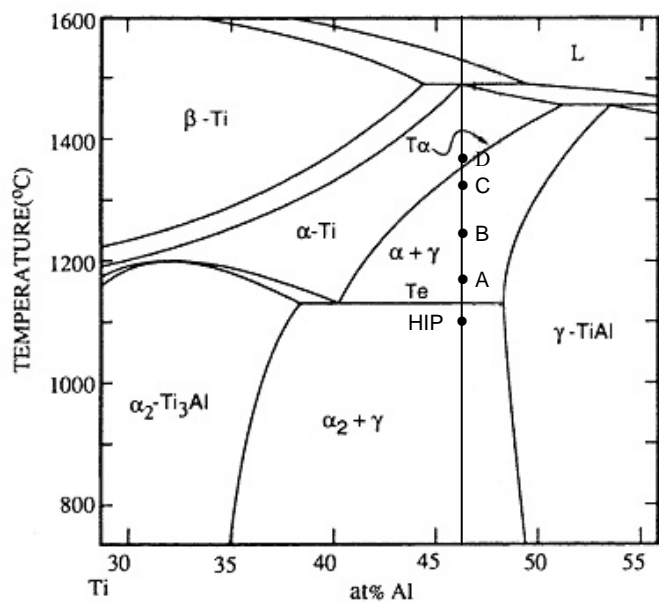


Figure 1

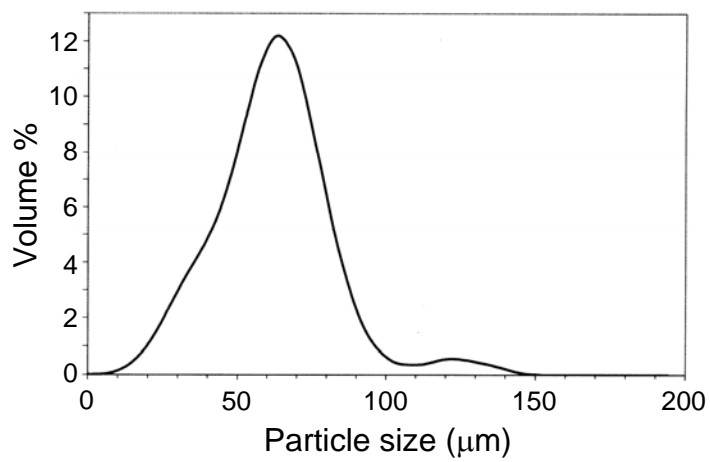


Figure 2

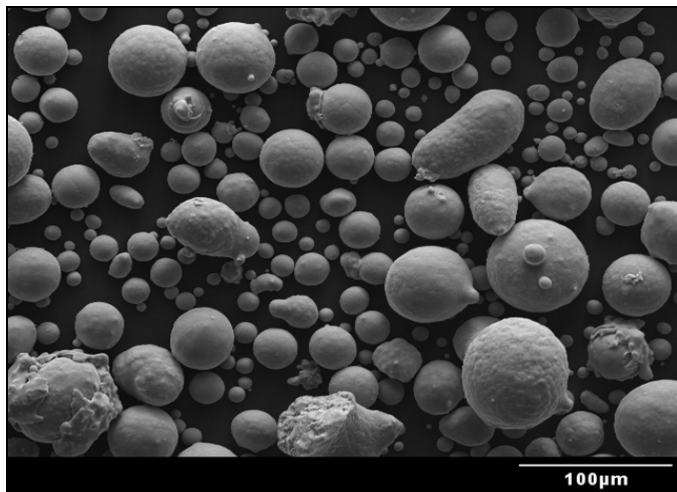


Figure 3

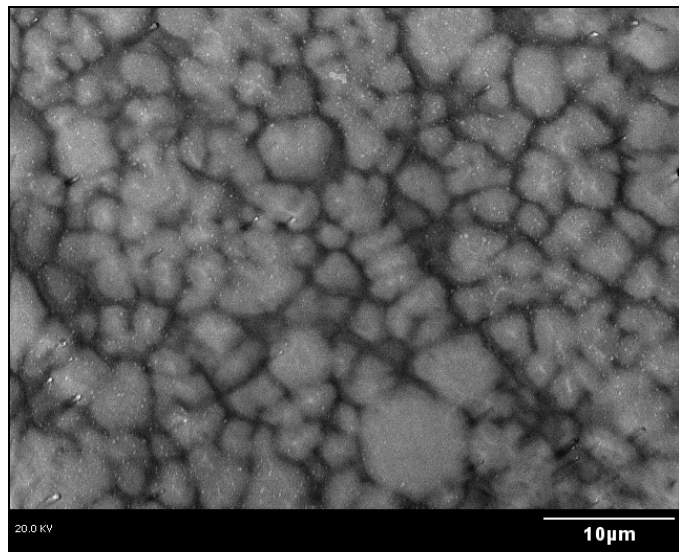


Figure 4

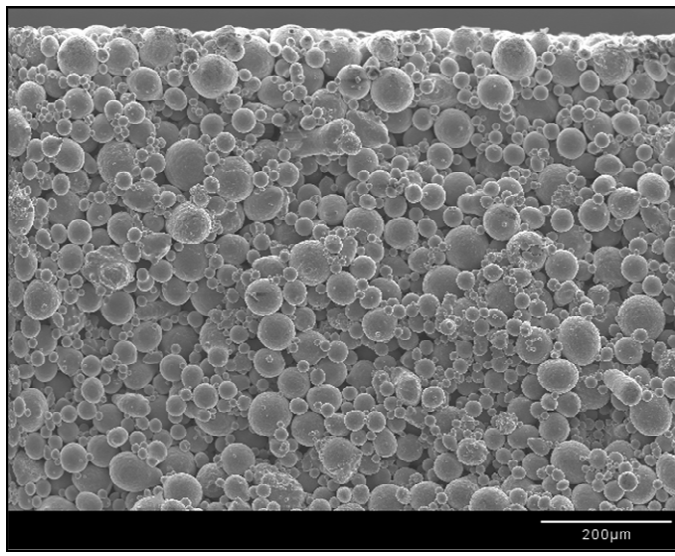


Figure 5



Figure 6(a), 6(b)

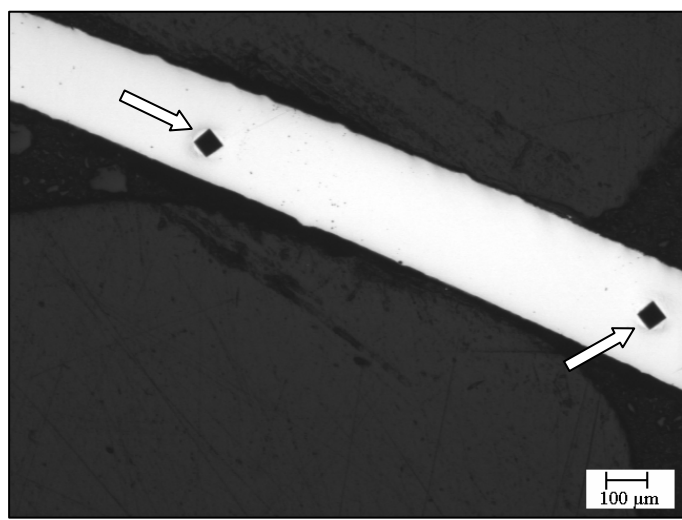


Figure 7

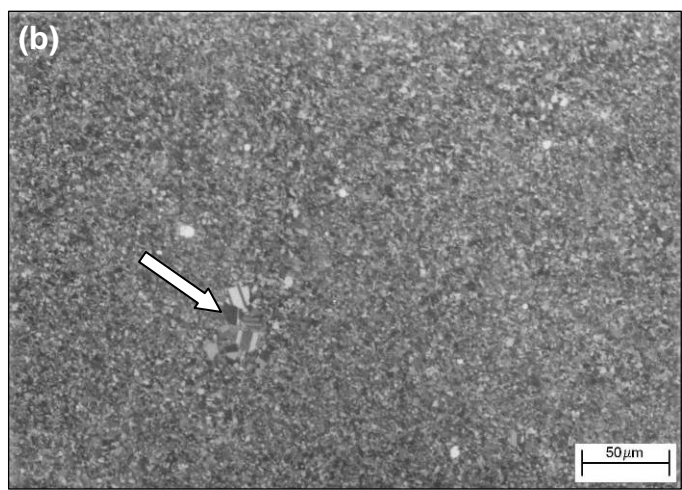
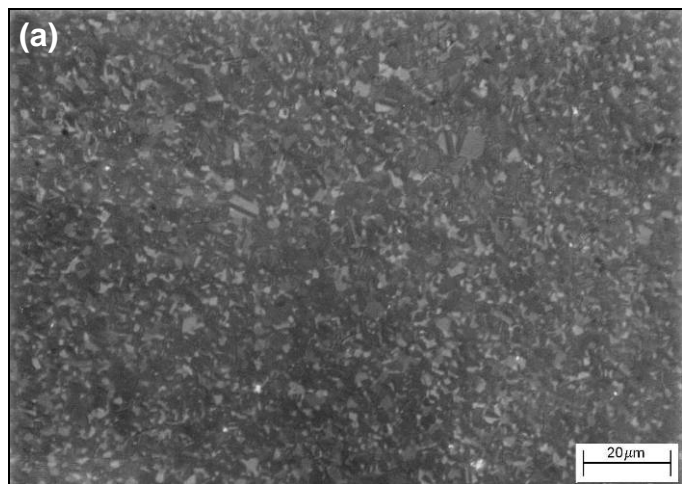


Figure 8(a), 8(b)

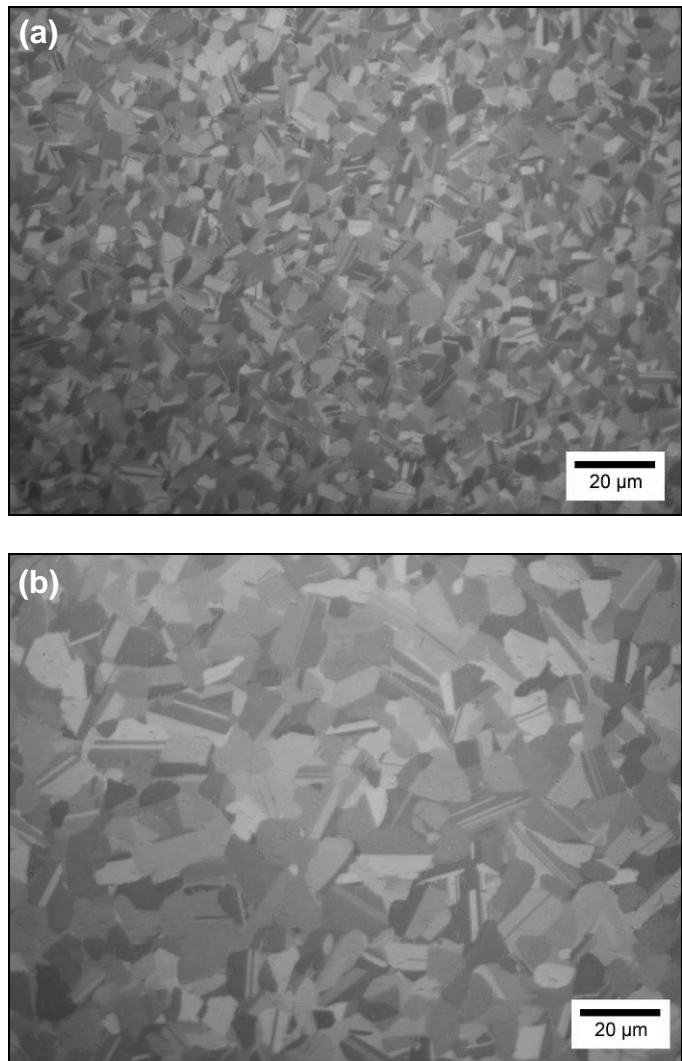


Figure 9(a) and 9(b)

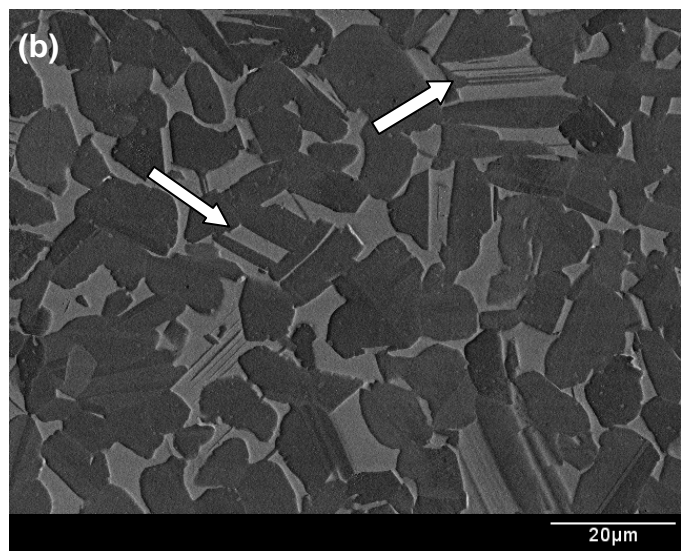
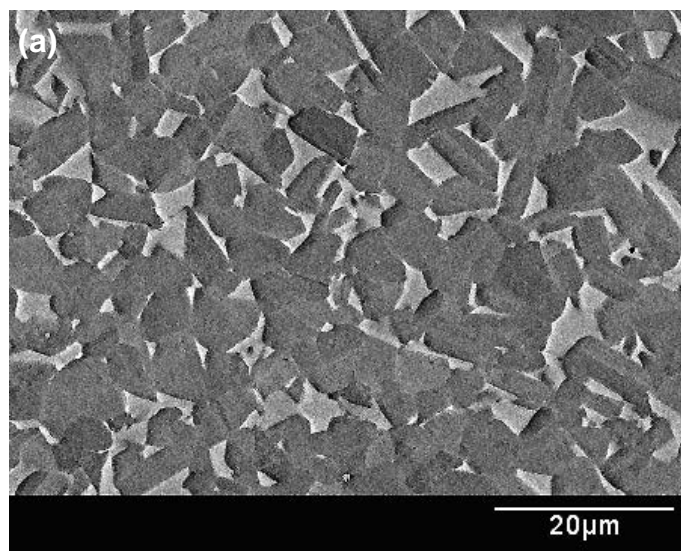


Figure 10(a), 10(b)

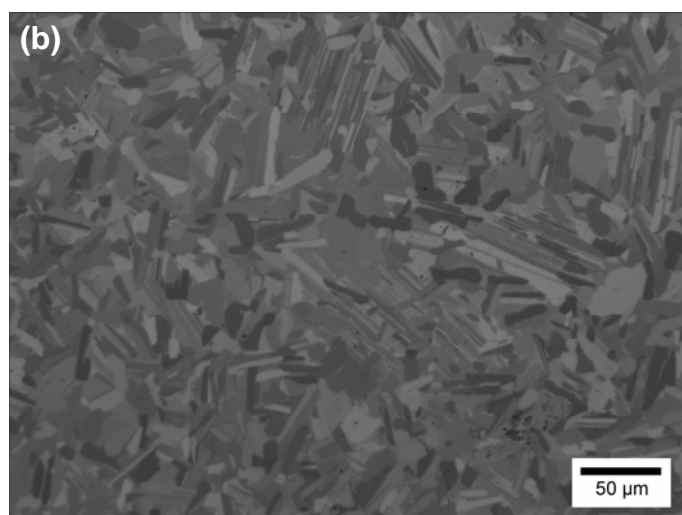
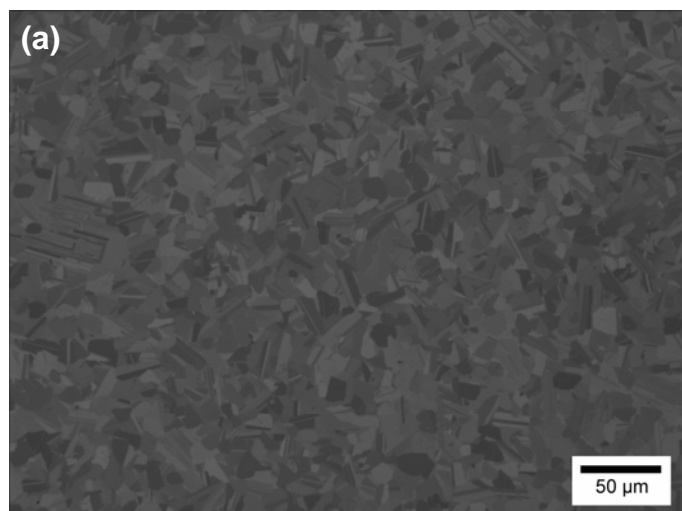


Figure 11(a), 11(b)

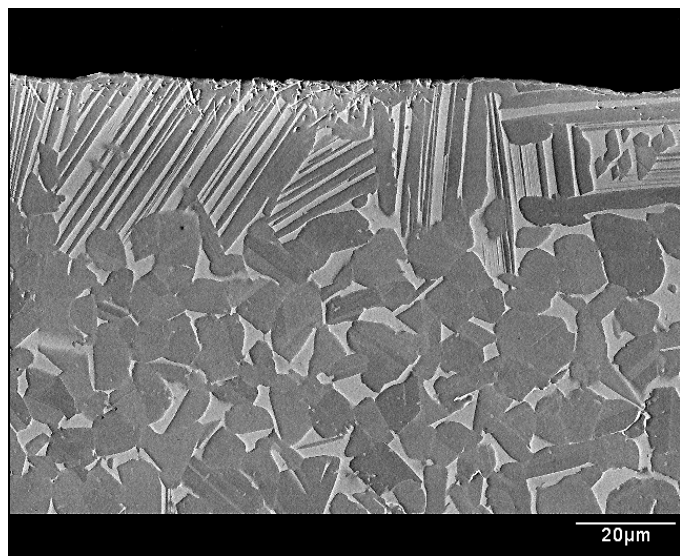


Figure 12